Distinction between Perceptual and Attentional Processing in Working Memory Tasks: A Study of Phase-locked and Induced Oscillatory Brain Dynamics

Marie-Pierre Deiber[1,2], Pascal Missonnier[1], Olivier Bertrand[3], Gabriel Gold[1], Lara Fazio-Costa[1], Vicente Ibañez[1], and Panteleimon Giannakopoulos[1,4]

Abstract

■ Working memory involves the short-term storage and manipulation of information necessary for cognitive performance, including comprehension, learning, reasoning and planning. Although electroencephalogram (EEG) rhythms are modulated during working memory, the temporal relationship of EEG oscillations with the eliciting event has not been well studied. In particular, the dynamics of the neural network supporting memory processes may be best captured in induced oscillations, characterized by a loose temporal link with the stimulus. In order to differentiate induced from evoked functional processes, the present study proposes a time–frequency analysis of the 3 to 30 Hz EEG oscillatory activity in a verbal *n*-back working memory paradigm. Control tasks were designed to identify oscillatory activity related to stimulus presentation (passive task) and focused attention to the stimulus (detection task). Evoked theta activity (4–8 Hz) phase-locked to the visual stimulus was evidenced in the parieto-occipital region for all tasks. In parallel, induced theta activity was recorded in the frontal region for detection and *n*-back memory tasks, but not for the passive task, suggesting its dependency on focused attention to the stimulus. Sustained induced oscillatory activity was identified in relation to working memory in the theta and beta (15–25 Hz) frequency bands, larger for the highest memory load. Its late occurrence limited to nonmatched items suggests that it could be related to item retention and active maintenance for further task requirements. Induced theta and beta activities displayed respectively a frontal and parietal topographical distribution, providing further functional information on the fronto-posterior network supporting working memory. ■

INTRODUCTION

Working memory refers to the set of memory stores and control processes that enable us to hold and manipulate incoming information for several seconds in the context of a cognitive activity. Functional neuroimaging literature indicates that tasks requiring working memory activate a functional network linking regions of the prefrontal cortex with posterior association cortices (Baddeley, 1998; Cohen et al., 1997; Courtney, Ungerleider, Keil, & Haxby, 1997; Manoach et al., 1997). However, the question of how the brain integrates different groups of neurons into a network supporting working memory functions is largely debated. The cerebral oscillatory activity recorded with electroencephalography or magnetoencephalography (EEG/MEG) has aroused growing interest as a potential functional support for such a network. Several recent contributions have reported the reactivity of specific EEG frequency bands to various memory paradigms. Theta frequency (4–8 Hz) has been thought to reflect cortico-hippocampal interactions necessary for memory performance (Newman, & Grace, 1999; Miller, 1991). An increase of frontal theta power with working memory load has been often described, although the temporal course and topographic distribution of the theta effect vary across reports (Onton, Delorme, & Makeig, 2005; Jensen, & Tesche, 2002; Raghavachari et al., 2001; Krause et al., 2000; Kahana, Sekuler, Caplan, Kirschen, & Madsen, 1999; Gevins, Smith, McEvoy, & Yu, 1997). Oscillations at alpha frequency (8–12 Hz), associated with thalamocortical interactions, are modulated by alertness and cognitive processes such as attention and memory (Babiloni et al., 2004; Klimesch, 1999). Alpha reactivity to working memory remains highly controversial, with findings reporting a decrease or increase of alpha power during memory tasks (for review, Jensen, Gelfand, Kounios, & Lisman, 2002; Klimesch,

[1]University Hospitals of Geneva, Switzerland, [2]INSERM E340, La Tronche, France, [3]INSERM U280, Bron Cedex, France, [4]University Hospitals of Lausanne, Prilly, Switzerland

1999). Analyses of beta frequency (15–30 Hz) during memory activation are still scarce, but suggest that beta oscillations are modulated during item rehearsal in working memory (Onton et al., 2005; Tallon-Baudry, Bertrand, & Fischer, 2001; Tallon-Baudry, Bertrand, Peronnet, & Pernier, 1998). In contrast to the disparity of data within the frequency range below 30 Hz, numerous reports focusing on gamma oscillations (30–100 Hz) demonstrate their correlation with various cognitive functions, including short-term memory maintenance (Gruber, Tsivilis, Montaldi, & Muller, 2004; Herrmann, Munk, & Engel, 2004; Howard et al., 2003; Sederberg, Kahana, Howard, Donner, & Madsen, 2003; Tallon-Baudry et al., 1998).

One main methodological issue rarely addressed in previous studies of working memory-related EEG/MEG rhythms is the distinction between evoked and induced brain oscillatory activities (Bastiaansen, & Hagoort, 2003). Evoked oscillatory activity bears a constant time and phase relationship with the eliciting event, whereas induced oscillatory activity characterized by a loose temporal relationship with the eliciting event is considered as the best candidate to yield information about the dynamics of cell assembly formation in the course of memory operations (Bastiaansen, & Hagoort, 2003; Tallon-Baudry, & Bertrand, 1999; Klimesch, Russegger, Doppelmayr, & Pachinger, 1998). Working memory not only includes encoding, retention, and recall of the memory items, but critically relies on integrative perception and selective attention to the incoming information (Jensen, & Tesche, 2002; Baddeley, 1998). Because the perceptual, attentional, and memory processes are likely to have distinct time and frequency relationships with the incoming stimulus, careful distinction between evoked and induced oscillatory activities in the time–frequency (TF) domain is essential to identify the neural substrates of the various components implicated in working memory.

Our study's aim was to distinguish evoked and induced oscillatory EEG activities, and examine their functional significance in the context of a verbal working memory paradigm. We used a TF analysis based on wavelet transform of the signal, which preserves both latency and frequency information of the event-related oscillatory bursts (Bastiaansen, & Hagoort, 2003; Tallon-Baudry, & Bertrand, 1999). The distinction between evoked and induced activities was performed by evaluating the phase locking of the EEG signal to the stimulus in the TF domain, through the computation of a phase-locking factor providing a reliable estimation of the evoked oscillatory activity (Tallon-Baudry, Bertrand, Delpuech, & Permier, 1997; Tallon-Baudry, Bertrand, Delpuech, & Pernier, 1996). Working memory *n*-back tasks were used, in which subjects were presented with a continuous stream of letters and had to indicate whether the displayed letter matched the one presented *n* positions back. In order to separate the oscillatory activities specifically linked to working memory from those related to concomitant stimulus-related perceptive and attentional processes, two control tasks were designed: (1) a passive viewing task of the letter series to examine the modulation of neural oscillations with stimulus presentation in the absence of any specific cognitive demand; and (2) a focused attention detection task to determine the respective contribution of attentional processes to working memory. Whereas modulations of beta and gamma oscillatory activities were previously reported during visual short-term memory (Tallon-Baudry et al., 2001; Tallon-Baudry et al., 1998), precise quantification of the EEG signal phase-locking and distinction of functions were not achieved. We focused on the 3–30 Hz frequency range, for which the signal phase-locking has not been systematically explored, in the attempt to elucidate which part of the theta, alpha, and beta oscillatory activities are related to stimulus processing, including selective attention, versus memory functions per se. While restraining the exploration of gamma oscillations more sensitive to noise, our methodological design using surface Laplacian estimates provided a precise topographical analysis of the 3–30 Hz oscillatory activities.

METHODS

Subjects

Eighteen healthy, cognitively intact right-handed volunteers (8 men, 10 women; 26.9 ± 2.6 years) participated in this study. All subjects were screened for normal or corrected-to-normal vision, and none reported a history of head injury, neurological or psychiatric disorders. All participants were medication free and none exhibited alcohol or drug abuse. Informed consent was obtained from all subjects. The study was approved by the Ethical Committee of the University Hospitals of Geneva, and was in line with the Declaration of Helsinki.

Procedure

The subjects, comfortably seated, watched a computer-controlled display screen at a distance of 57 cm. They viewed pseudorandom sequences of consonant and vowels common to the French alphabet, and pressed a computer-controlled button with their right index finger as soon as a target appeared (response trials). For non-target stimuli, no motor response was required (no-response trials). Stimuli consisted of white letters, Arial font (2° × 2.5° visual angle), with 10% gray noise, embedded in a 50% random noise gray rectangular background patch (6° × 6.7° visual angle). They were presented in the center of the screen for 0.5 sec, separated by 5-sec intervals (onset to onset) during which a dot helped subjects maintain fixation.

Three active tasks were tested, in which one third of the stimuli were targets (Figure 1). In the *detection task*,

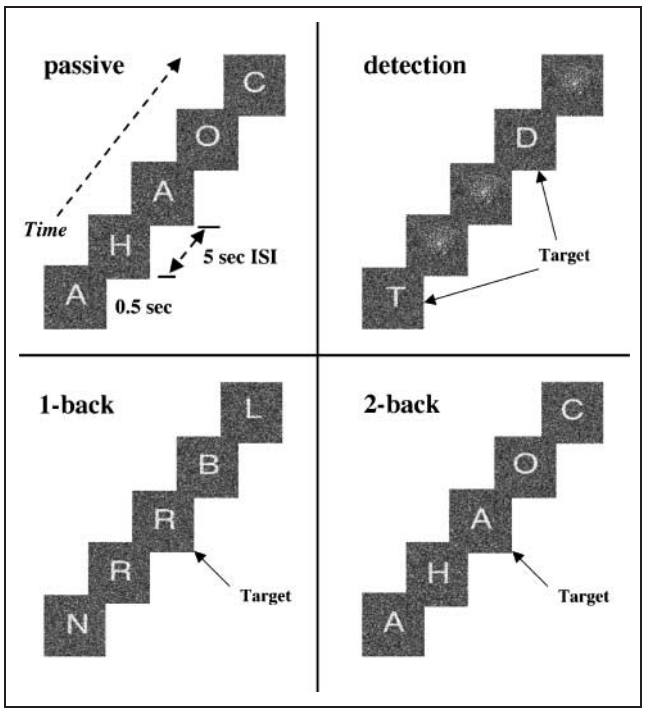

Figure 1. Schematic representation of the four tasks. Passive fixation task: letter series identical to the 2-back task. Detection task: response required at presentation of a letter. 1-back and 2-back tasks: response required when the letter is identical to the one presented one trial back (1-back task) or two trials back (2-back task). Stimulus duration = 0.5 sec, interstimulus interval (ISI) = 5 sec.

sequential letters (target) or background patches without letters (nontarget) were presented. In the *1-back task*, the target was any letter identical to the one immediately preceding it. In the *2-back task*, the target was any letter that was identical to the one presented two trials back. These three active tasks contained the comparison of stimulus-related information with memory contents, and working memory load increased from detection (minimally demanding) to 1-back (moderately demanding) and 2-back (highly demanding). To control for visual effects, an additional *passive task* was performed at the beginning of the recording session in the ultimate 11 of the 18 subjects (6 men, 5 women; 27.6 ± 2.1 years). In this passive task, letter series identical to the 2-back task were presented, but subjects were unaware of the nature of the task and watched the series passively. Each task was tested in three blocks (blocks 1, 2, 3) composed of 30 sequential stimuli each, adding up to 90 trials per task (active tasks: 21 response trials, 69 no-response trials). Subjects were informed about the nature of the forthcoming task right before each sequence. The order of task presentation was chosen to optimize the allocation of attentional resources for each task: passive task (blocks 1, 2, 3; in 11 subjects); detection (block 1); 1-back (block 1); 2-back (blocks 1, 2, 3); 1-back (blocks 2, 3); detection (blocks 2, 3). Reaction time (RT) and performance were systematically recorded, but no feedback on performance was provided. The absence of difference in RT and performance between blocks of the same task indicated that learning, habituation, and fatigue effects were minimal during the recording session.

Electrophysiological Recordings

Continuous EEG (Micromed, Brain Quick system 98, Treviso, Italy) was recorded using 20 surface electrodes referenced to the linked earlobes. Their locations, according to the 10-20 international system, were: Fp1, Fp2, F7, F3, Fz, F4, F8, T3, C3, Cz, C4, T4, T5, P3, Pz, P4, T6, O1, Oz, and O2. Skin impedance was kept below 5 kΩ. Electrophysiological signals were sampled at 1024 Hz with a lower cutoff of 0.3 Hz (DC amplifiers; Micromed). The electrooculogram was recorded using two pairs of bipolar electrodes in both vertical and horizontal directions. Single transistor–transistor logic (TTL) pulses synchronized with stimulus onset were recorded and used off-line to segment the continuous EEG data into epochs time-locked to stimulus onset.

Data Processing

In order to obtain a suitable number of trials for reliable TF analysis, EEG signals were corrected for ocular artifacts using a threshold reduction algorithm (NeuroScan; Compumedics, El Paso, TX), whose parameters were carefully selected in each individual to minimize any residual effects on the visually inspected EEG signal. The total analysis window was 5000 msec, starting 1500 msec before stimulus onset. Spatial resolution of EEG data was enhanced by surface Laplacian estimation performed on continuous EEG (regularized 3-D spline function, order 4). The Laplacian-transformed EEG trials were automatically scanned for contamination by muscular or electrode artifacts. Such Laplacian calculation acts as a high-pass spatial filter that reduces head volume conduction and cancels out reference electrode influence (Babiloni et al., 1996; Perrin, Bertrand, & Pernier, 1987). All subsequent analysis was performed on the Laplacian-transformed EEG signal ($\mu V/m^2$) computed at each electrode.

To detect and characterize the event-related EEG oscillations whose latency and frequency ranges are not known a priori, a method was chosen that preserves both types of information: the TF representation based on the wavelet transform of the signals (Tallon-Baudry et al., 1996, 1997, 1998). This method enables the analysis of stimulus-induced activities, which appear with a jitter in latency from one trial to the next, and thus, tend to disappear on the classic averaged evoked potential. Computation of the TF energy on each single trial and averaging (TF energy averaged across single trials) provides information on both evoked (stimulus phase-

locked) and induced (non-phase-locked) activities, providing their signal-to-noise ratio is high enough. A ''phase-averaging'' technique is proposed to quantify the level of stimulus phase-locking of oscillatory activities, irrespective of their amplitude (Tallon-Baudry et al., 1996, 1997).

The signal was convoluted by complex Morlet's wavelets $w(t, f_0)$ (Kronland-Martinet, Morlet, & Grossmann, 1987) having a Gaussian shape both in the time domain (*SD* σ_t) and in the frequency domain (*SD* σ_f) around its central frequency f_0: $w(t, f_0) = A.\exp(-t^2/2\sigma^2_t) \times \exp(2i\pi f_0 t)$, with $\sigma_f = 1/2\pi\sigma_t$. Wavelets were normalized so that their total energy was 1. A wavelet family is characterized by a constant ratio (f_0/σ_f), which should be chosen in practice greater than ~5 (Grossmann, Kronland-Martinet, & Morlet, 1989). We used a wavelet family defined by $f_0/\sigma_f = 10$, with f_0 ranging from 3 to 30 Hz in 1-Hz steps. At 6 Hz, this leads to a wavelet duration ($2\sigma_t$) of 530 msec and to a spectral bandwidth ($2\sigma_f$) of 1.2 Hz, and at 20 Hz, to a wavelet duration of 159 msec and to a spectral bandwidth of 4 Hz. The time resolution of this method thus increases with frequency, whereas the frequency resolution decreases. The time-varying energy $E(t, f_0)$ of the signal in a frequency band around f_0 is the squared norm of the result of the convolution of a complex wavelet $w(t, f_0)$ with the signal $s(t)$: $E(t, f_0) = |w(t, f_0) * s(t)|^2$. A family of wavelets will provide a TF representation of the energy of the signal (TF energy). By averaging the TF energy of each single trials, both phase-locked and non-phase-locked activities are summed. The mean TF energy of the prestimulus period (between 1100 and 100 msec before stimulus onset) is considered as a baseline level and subtracted from the prestimulus and poststimulus TF energy. This correction is done separately in each frequency band.

The stimulus phase-locking of the oscillatory activity can be evaluated in the TF domain by adapting the ''phase-averaging'' methods previously proposed in the frequency domain by Jervis, Nichols, Johnson, Allen, and Hudson (1983). We consider the normalized complex time-varying energy of each single trial i: $P_i(t, f_0) = w(t, f_0) \cdot s_i(t)/ |w(t, f_0) \cdot s_i(t)|$. Averaging these quantities across single trials leads to a complex value related to the phase distribution of each TF region around t and f_0. The modulus of this value is called the ''phase-locking factor.'' It ranges from 0 (purely non-phase-locked activity) to 1 (strictly phase-locked activity). This method, shown to be robust against artifacts, can identify even very low amplitude signals provided they are rather strictly phase-locked. To detect phase ordering, the Rayleigh statistical test of uniformity of angle is used (Jervis et al., 1983).

Data Analysis

On average, 49 correct no-response trials, 17 correct response trials, and 63 passive trials were analyzed per condition and subject after artifact rejection. Because of the high subject performance level, there were not enough incorrect trials to analyze them. Response and no-response trials were processed separately to analyze the cerebral activity related to matched and nonmatched responses, respectively. A broad frequency range from 3 to 30 Hz was examined, including theta, alpha, and beta frequency ranges. All signal analyses were performed with the ELAN-Pack software developed at INSERM U280 (Lyon, France, www.lyon.inserm.fr/280).

Because the data were not normally distributed, the nonparametric Quade test for related samples and Conover procedures as post hoc tests of significance (Conover, 1980) were applied to TF data (Tallon-Baudry et al., 1996, 1997). This test is an adaptation of the Wilcoxon signed-ranks test to the case of several related samples, performed by ranking data paired by subjects. When a significant global effect of the tested conditions is present, Conover procedures can compare all possible combinations of experimental condition pairs, and determine in which pairs significant differences occur. The Quade test was performed separately for theta, alpha, and beta frequency bands. To reduce the effect of intersubject variability in frequency and latency, as well as the number of statistical comparisons, the test was applied to mean TF energy values within smoothing TF windows regularly shifted by 50 msec to cover the entire analysis time window. According to the principle of wavelet analysis, the size of the smoothing TF windows differed with the frequency band of interest, varying from long duration and narrow bandwidth in the theta range to shorter duration and larger bandwidth in the beta range. Theta: 600 msec × 4 Hz smoothing window centered at 6 Hz (frequency range 4–8 Hz); alpha: 400 msec × 4 Hz smoothing window centered at 10 Hz (frequency range: 8–12 Hz); beta: 250 msec × 10 Hz smoothing window centered at 20 Hz (frequency range: 15–25 Hz). The significance level of $p < .01$ was retained for both Quade and Conover tests after Bonferroni correction for multiple tests.

Influence of cognitive demand on oscillatory activity was assessed by nonparametric Quade analysis of the three active conditions in the 18 subjects, with task (detection, 1-back, 2-back) as a within-subject factor. The detection task engaged primarily focused attention with minimal memory component, whereas the *n*-back tasks engaged working memory of varying load. Separate analysis was performed for response and no-response trials, as they could potentially engage distinct neural processes. In order to evaluate more generally the cerebral resources engaged in active tasks as compared to passive viewing, and to identify the cerebral oscillatory pattern related to motor activity in response trials, additional statistical analysis was performed with inclusion of the passive task in the subgroup of 11 subjects, with task (passive, detection, 1-back, 2-back) as a within-subject factor.

RESULTS

Performance and Event-related Potentials

Subjects performed very satisfactorily in the three active tasks, with a minimum of 88.9% of correct responses. On average, performance was correct at 99.5% in detection, 98.9% in 1-back, and 96.9% in 2-back tasks. The task had a significant effect on performance (Friedman test, $p < .01$), subjects performing better in the detection and 1-back tasks than in the 2-back task (Wilcoxon matched-pairs test, $p < .01$ and $p < .05$, respectively).

RT increased with task difficulty, being shorter in the detection task (675 ± 96 msec), intermediate in the 1-back task (727 ± 112 msec), and longer in the 2-back task (837 ± 177 msec). Repeated-measures analysis of variance (ANOVA) showed a highly significant task effect on RT [$F(2,34) = 17.7$, $p < .0001$]. Contrast analysis revealed that RT was significantly different across the three tasks, being shorter in the detection task than in the 1-back and 2-back tasks [$F(1,17) = 24.6$ and $F(1,17) = 21.3$, $p < .0001$, respectively] and shorter in the 1-back than in the 2-back task [$F(1,17) = 12.4$, $p < .005$].

The event-related potentials (ERPs) are displayed in Figure 2 for each task, illustrating the early visual evoked components culminating at occipital and parietal sites. The P1 (102 msec) and N1 (155 msec) were similar in all tasks. An OFF response was present at occipital electrodes at 585 msec (i.e., 85 msec after stimulus offset). Over all electrodes, the ERPs returned to baseline within 1000 to 2000 msec after stimulus onset. Differences between tasks occurring on P2 and N2 components have been described elsewhere (Missonnier et al., 2003).

Theta Frequency Band (4–8 Hz)

Transient Theta Activity

The representation of TF energy averaged across single trials showed the existence of a transient energy increase in the theta frequency range between 0 and 1000 msec (Figure 3), present for both response and no-response trials. This transient activity was of maximal amplitude at the frontal electrode Fz at ~400 msec, but it was also present at parietal electrodes (Pz), where it peaked earlier (~170 msec). The topographical distribution of energy in the 4–8 Hz frequency range displayed distinct parieto-occipital and frontal transient theta activity (Figure 4C). The TF representation of the phase-locking factor showed a phase-locked component peaking at 275 msec, on average (Figure 3), with statistical significance at Pz (Rayleigh test, $p < .001$) as well as at Fz ($p < .01$). In contrast to the averaged TF energy, the phase-locking factor was of larger amplitude at Pz than at Fz (Figure 3; one-way ANOVA, main effect of electrode, all tasks confounded: $F = 14.8$, $p < .005$). We compared the latency of TF energy and phase-locking factor culmination peaks at Fz and Pz electrodes, respectively. Although there was no significant difference at Pz (paired t test, $t = 1.297$, $p = .21$), the phase-locking factor peaked significantly earlier than the TF energy at Fz ($t = -5.152$, $p < .0001$).

At frontal electrodes, the amplitude of theta energy was similar among the three active tasks, whereas it was much weaker in the passive task (Figure 3). This contrasted with the parietal electrodes, where theta energy amplitude was comparable across all tasks. The energy profile in the 4–8 Hz range revealed a transient theta component in both response and no-response trials, of larger amplitude and peaking later at Fz as compared to Pz (Figure 4A and B). Moreover, the theta component was hardly present in the passive task at Fz (Figure 4A–C). The Quade test (passive, detection, 1-back, 2-back; $n = 11$), performed separately on averaged TF energy of both trial types, confirmed a significant task effect on the theta transient component restricted at Fz, Fp1, and Fp2 electrodes. The maximal effect occurred at Fz between 51 and 660 msec, and the Conover procedures revealed significant differences between each active task and the passive task in this time window, but no significant difference between the three active tasks.

Sustained Theta Activity

Although the early transient theta component was equally present in response and no-response trials, the TF representation revealed that frontal theta energy remained of high amplitude later in the delay for no-response trials (Figure 3). This sustained frontal energy was absent in the representation of the phase-locking factor (Figure 3), indicating that it was not phase-locked to stimulus onset. Moreover, the sustained theta component, which displayed a frontopolar distribution, appeared of higher amplitude in the 2-back task within the whole 4- to 8-Hz range (Figures 3 and 4A,C). The Quade test (detection, 1-back, 2-back; $n = 18$) confirmed a significant task effect on TF energy at frontopolar Fp2 and frontal F3, Fz, F4, and F7 electrodes between 965 and 2390 msec. At these electrodes, TF energy in the 2-back was higher than in the detection task. At electrodes Fz and F4, TF energy in the 2-back was also higher than in the 1-back task.

Alpha Frequency Band (8–12 Hz)

In the 8–12 Hz frequency range, the TF representation of energy averaged across single trials revealed a long lasting decrease in energy between −500 and 1500 msec, followed by a short increase peaking at ~2500 msec (Figure 5). These modulations of TF energy were present in both response and no-response trials and were maximal at parietal sites. The TF representation of the phase-locking factor showed a significant phase-locked

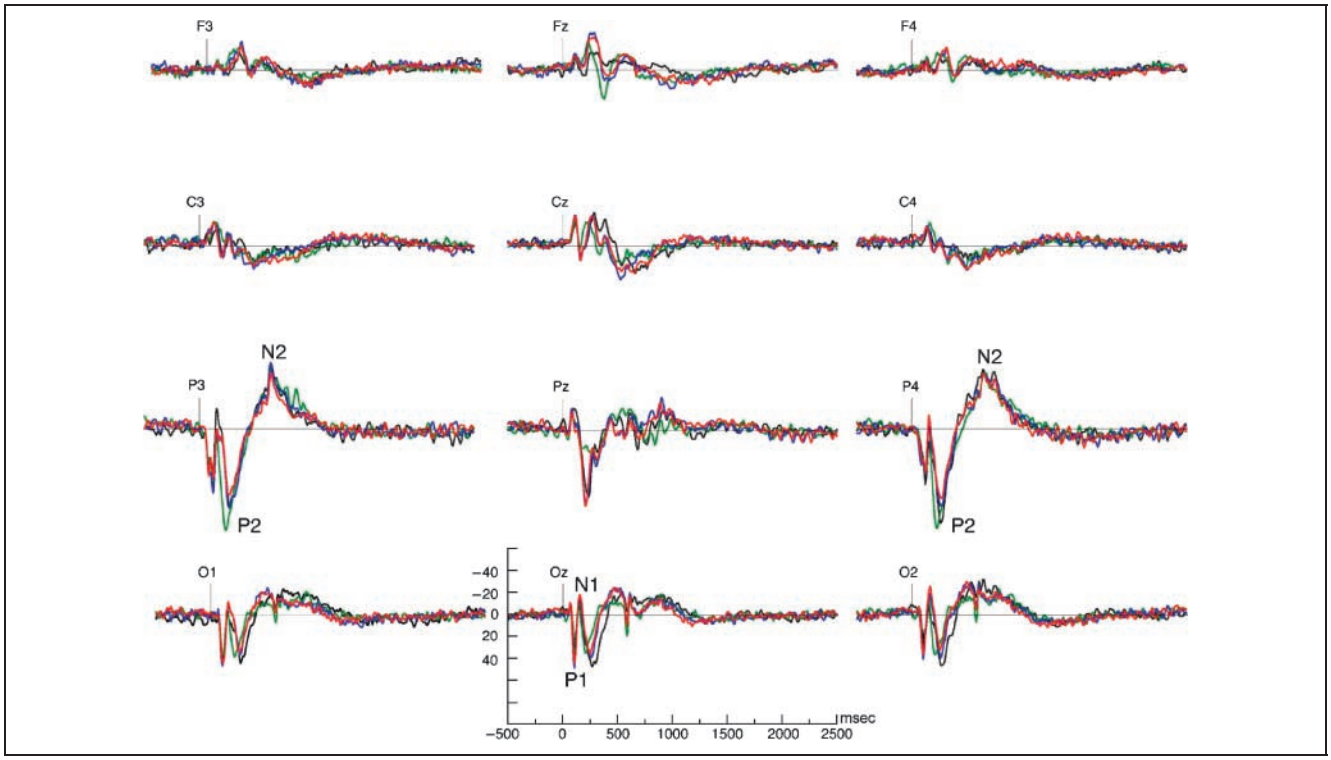

Figure 2. Grand-average ERP waveforms for no-response trials in each task. The P1–N1 complex is similar in all tasks. At occipital sites, an OFF response appears as a downward inflection at 585 msec. Waveforms return to baseline between 1000 and 2000 msec with no evidence of sustained potential during the delay. Black: passive; green: detection; blue: 1-back; red: 2-back. Amplitude units: $\mu V/m^2$.

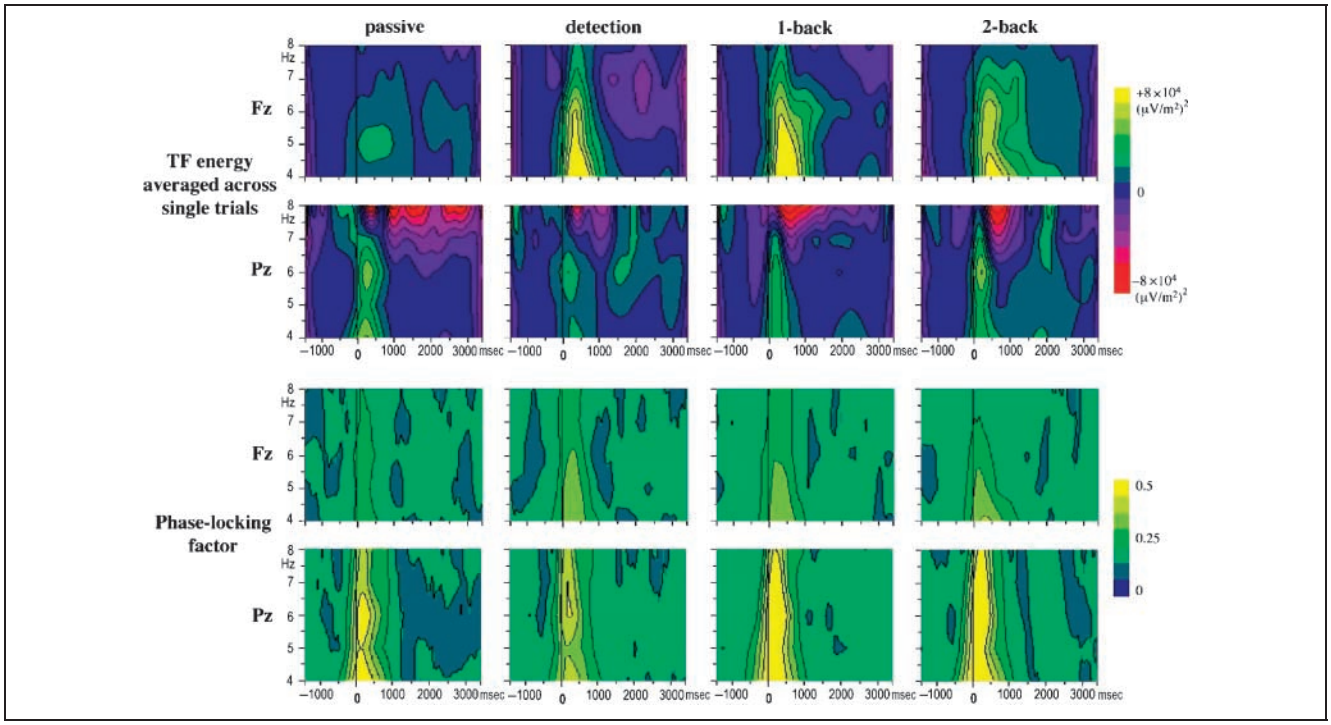

Figure 3. Time–frequency (TF) analysis in the theta frequency range (4–8 Hz) at electrodes Fz and Pz, grand-average across subjects. *Upper two rows:* TF energy averaged across single no-response trials (combination of phase-locked and non-phase-locked activities). Results are baseline corrected (−1100 to −100 msec), producing negative and positive values. There is a transient theta component of largest amplitude at Fz (400 msec). In the 2-back task, the energy remains sustained at Fz (1250–2500 msec). *Lower two rows:* Phase-locking factor. Values >0.29 denote significant stimulus phase-locking (Rayleigh test, $p < .01$). The transient theta component is largely phase-locked to stimulus onset at Pz electrode, less so at Fz electrode. The sustained theta component (2-back task) is not stimulus phase-locked.

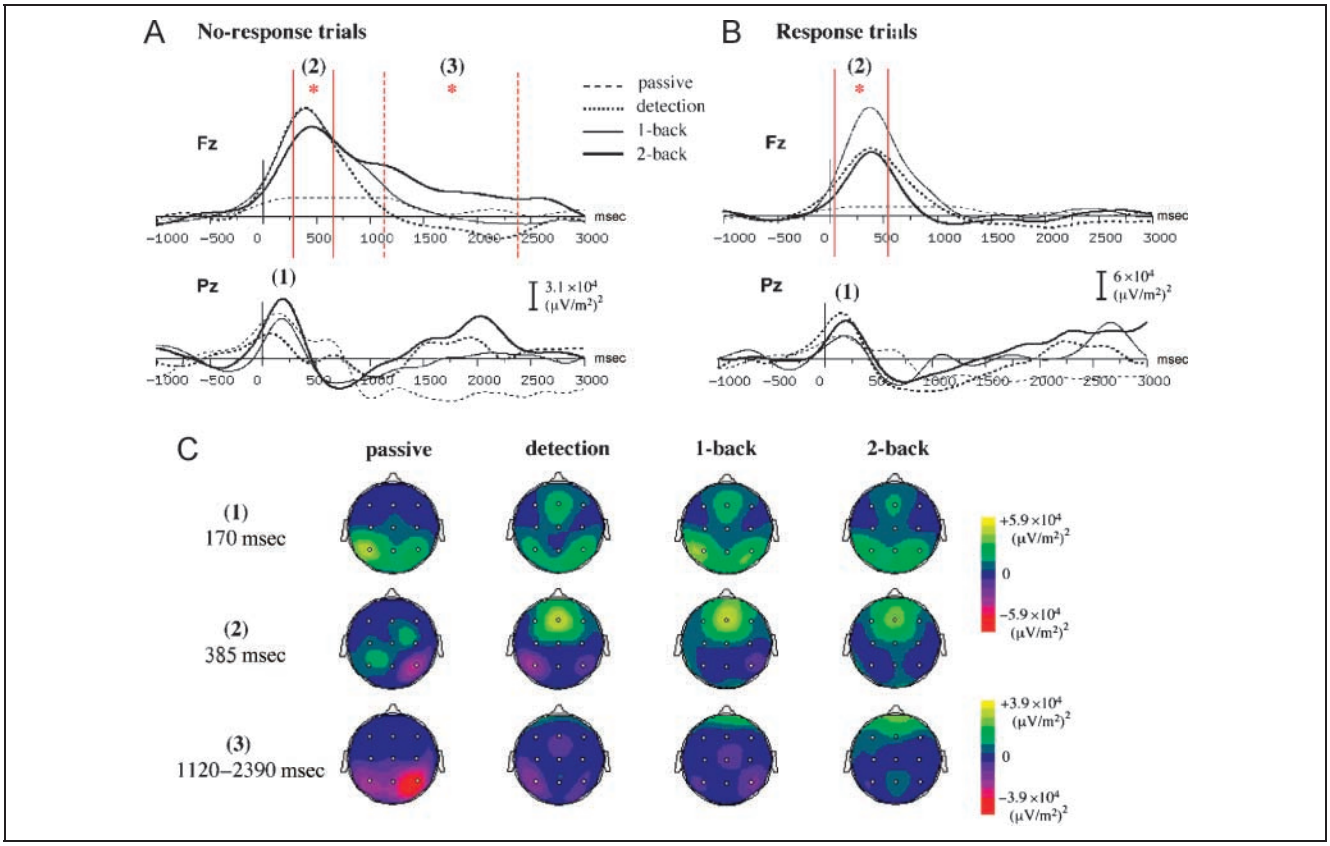

Figure 4. (A, B) Theta frequency band profile (4–8 Hz) of TF energy averaged across no-response (A) and response (B) single trials, at electrodes Fz and Pz (grand-average across subjects). Red vertical lines indicate the time windows of significance of the Quade test (*$p < .01$): continuous lines for Quade test on four tasks (passive, detection, 1-back, 2-back), dashed lines for Quade test on three active tasks (detection, 1-back, 2-back). For both response and no-response trials, the transient theta component is of larger amplitude and peaks later at Fz (2) than at Pz (1). At Fz, it is significantly larger in each active task as compared to the passive task, whereas no task effect is observed at Pz. The sustained theta component (3) is only observed in no-response trials and is larger in the 2-back task. (C) Topographic maps of TF energy averaged across single no-response trials in the 4–8 Hz frequency range. (1) Maps at 170 msec, peak of the transient theta component at Pz; the frontal increase of energy is already visible in the three active tasks. (2) Maps at 385 msec, peak of the transient theta component at Fz; it is comparable between the three active tasks, but absent in the passive task. (3) Mean maps between 1120 and 2390 msec (Quade significance at Fz), showing the anterior distribution of the sustained theta component larger in the 2-back task.

alpha component at posterior electrode sites, lasting for 1000 msec after stimulus onset (Rayleigh test, $p < .01$; Figure 5). No significant difference in TF energy was observed in the alpha frequency range between the three active tasks (Figure 5). In contrast, the decrease of TF energy in response trials was significantly larger for each active task compared to the passive task at electrodes C3 and C4 between 355 and 1015 msec (Figure 7A,B). The central topography of TF energy difference between the three pooled active tasks and the passive task was compatible with modulation of the alpha rhythm related to cerebral motor activity (Figure 7C).

Beta Frequency Band (15–25 Hz)

In the 15–25 Hz frequency range, the TF representation of energy averaged across single trials revealed a decrease in energy at 0–500 msec, followed by a sharp increase at 700–1000 msec (Figure 5), these variations being maximal at parietal sites and present for both response and no-response trials. Beta energy remained of sustained amplitude during the delay (Figures 5 and 6A). In the passive task, beta power increase was less sharp than in the active tasks, and remained of smaller amplitude (Figures 5 and 6A). Observation of the phase-locking factor showed a significant phase-locked beta component following onset and, to a lesser degree, offset of the stimulus on posterior electrode sites (Rayleigh test, $p < .01$; Figure 5). The sustained beta component did not appear on the representation of the phase-locking factor, indicating that it was not phase-locked to the stimulus. The energy profile in the 15–25 Hz range revealed that response and no-response trials displayed task-related differences in beta reactivity (Figure 6A). The three active tasks elicited a similar parietal beta power time course in response trials, whereas they had a differential effect in no-response trials, with two characteristics (Figure 6A,B): (1) parietal beta power increased and peaked earlier in the detection task

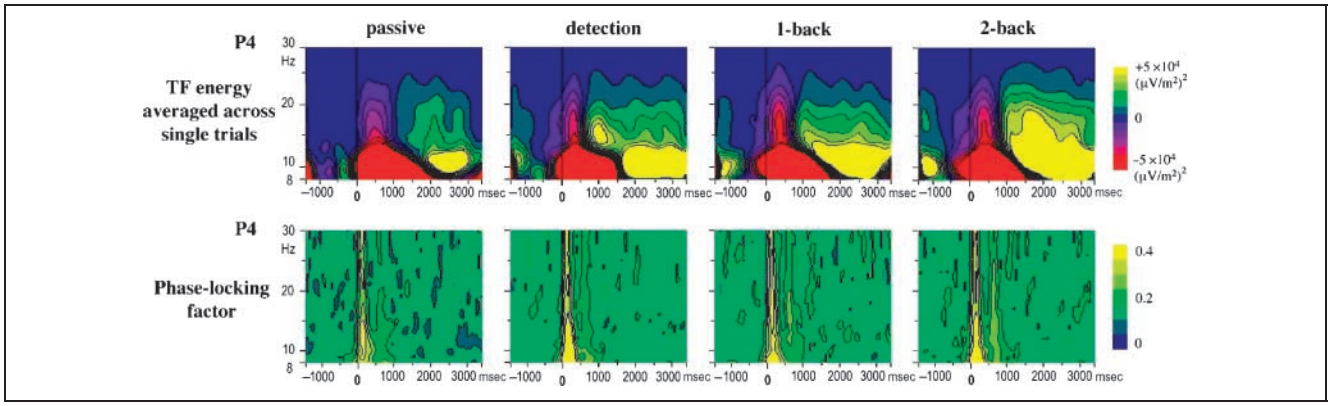

Figure 5. TF analysis in the alpha and beta frequency ranges (8–30 Hz) at electrode P4, grand-average across subjects. Top: TF energy averaged across single no-response trials and baseline corrected. In the three active tasks, there is a decrease in energy after stimulus onset (red), lasting longer in the alpha range (8–12 Hz) and followed by a short rebound (yellow). In the beta range (15–25 Hz), there is a sustained energy increase lasting during the delay and more pronounced in the 2-back task. Bottom: Phase-locking factor. Values > 0.29 denote significant stimulus phase-locking (Rayleigh test, $p < .01$). It is of large amplitude at onset of stimulus and smaller at stimulus offset. The sustained beta component is not stimulus phase-locked.

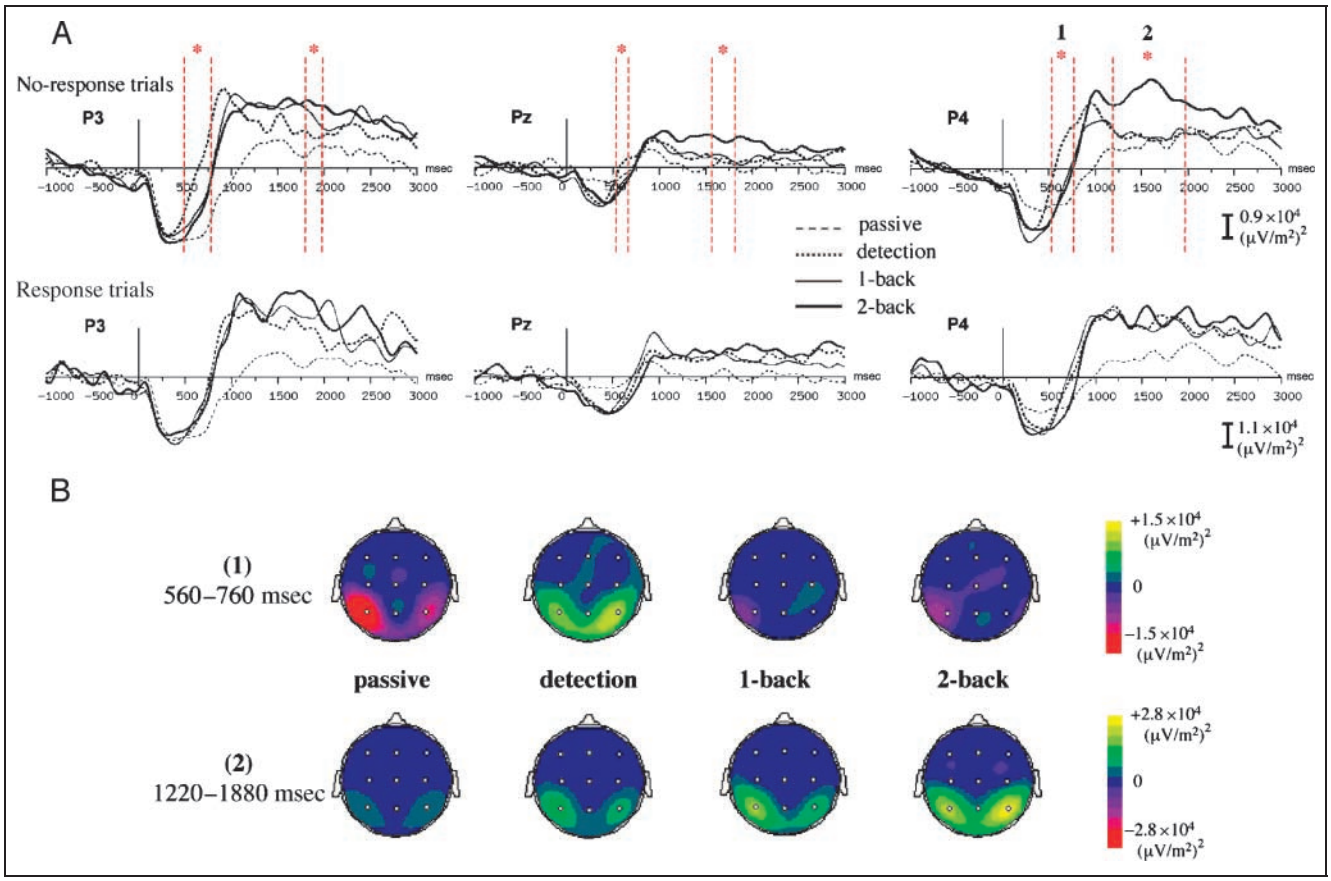

Figure 6. (A) Beta frequency band profile (15–25 Hz) of TF energy averaged across single no-response (first row) and response trials (second row), at parietal electrodes P3, Pz, and P4. Vertical dashed lines indicate the time windows of significance of the Quade test performed on the three active tasks (detection, 1-back, 2-back; $*p < .01$). For the no-response trials only, the three active tasks are significantly different at two distinct time periods: in the first time period (1), the difference is due to the earlier rise of beta power in the detection task; in the second time period (2), it is due to a larger beta power in the 2-back task. (B) Topographic maps of TF energy averaged across single no-response trials in the 15–25 Hz frequency range, in time windows corresponding to Quade significance at P4. (1) Mean maps between 560 and 760 msec showing the early beta component in the detection task posteriorly distributed; (2) Mean maps between 1220 and 1880 msec showing the parietal distribution of the beta sustained component. It is of larger amplitude in the 2-back task, essentially in the right parietal region.

as compared to the *n*-back tasks; (2) sustained parietal beta power was larger in the 2-back task, and this was even more striking in the right posterior region.

No-response Trials

The Quade test performed on the four tasks (passive, detection, 1-back, 2-back; $n = 11$) showed a significant centro-parietal difference across tasks between 610 and 1066 msec, and the Conover procedures revealed that it was due to the earlier and larger beta synchronization in each active task as compared to the passive task. The Quade test performed on the three active tasks (detection, 1-back, 2-back; $n = 18$) showed a first significant parieto-occipital difference across active conditions between 510 and 860 msec (Figure 6A). This difference was due to the earlier beta synchronization in the detection task as compared to the 1-back and 2-back tasks at parietal and occipital electrodes (Figure 6B). A second significant difference in beta energy across active conditions was revealed between 1220 and 2200 msec (Figure 6A), with a significantly larger amplitude of sustained beta energy in the 2-back as compared to the detection task at P3, Pz, P4, T6, O2, and Oz electrodes (Figure 6B). Additionally at P4 and T6 electrodes, beta energy was larger in the 2-back than in the 1-back task. No significant difference was found between 1-back and detection tasks.

Response Trials

Observation of the TF representation of beta energy averaged across single response trials showed a large energy decrease in the central region, contralateral to the responding hand, at around 500 msec in the three active tasks, but not in the passive task (Figure 7A).

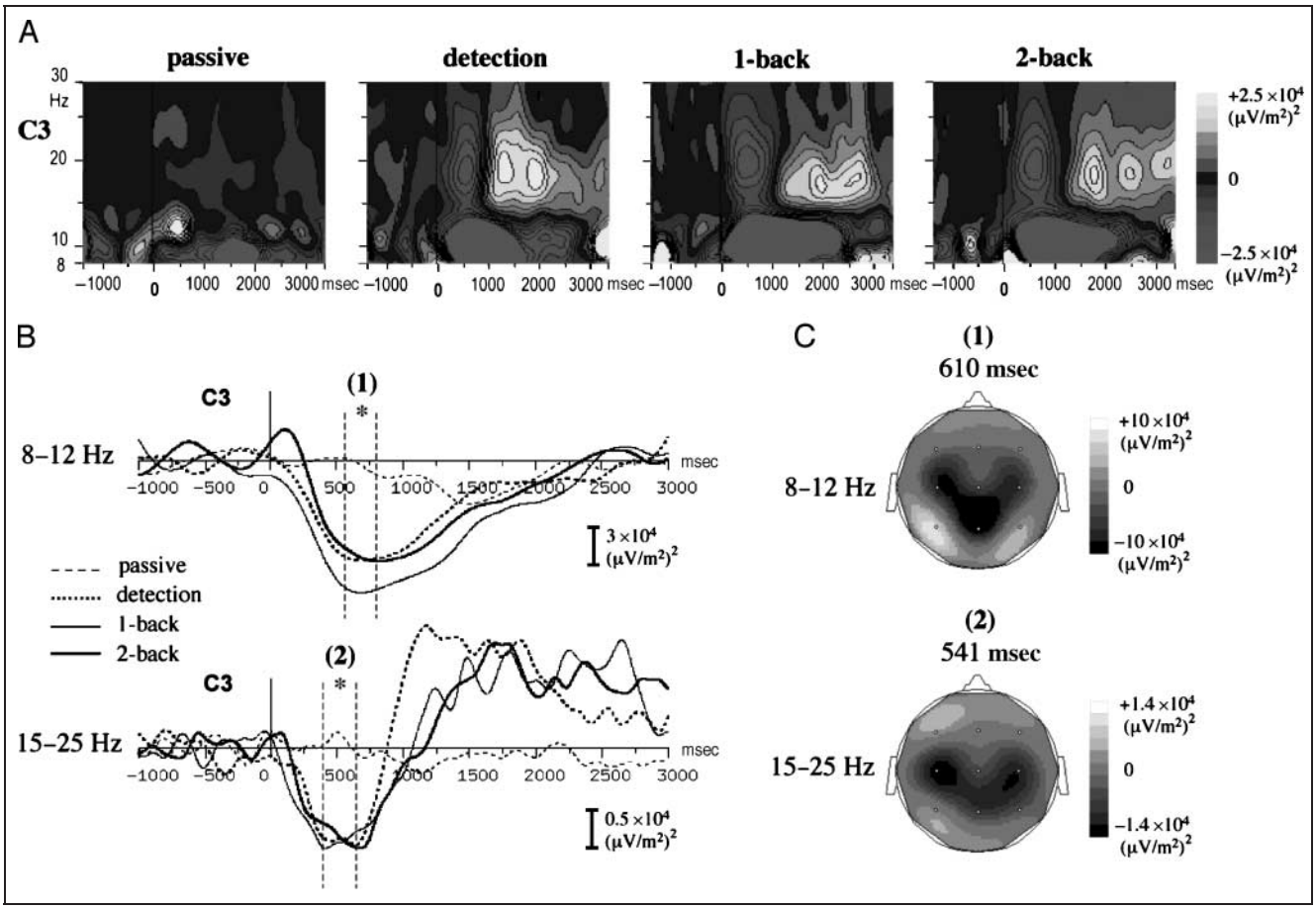

Figure 7. (A) TF analysis in the alpha and beta frequency ranges at electrode C3 (8–30 Hz), averaged across all single trials for the passive task and single response trials for the three active tasks. In the three active tasks, the alpha and beta energy decreases after stimulus onset (gray), the decrease lasting longer in the alpha range while a rebound of beta energy is observed (white). There is less energy variation in the passive task in the same time period. (B) Frequency band profiles in the 8–12 Hz range (top) and 15–25 Hz range (bottom) of TF energy averaged across all single trials for the passive task and single response trials for the three active tasks, at electrode C3. The decrease of alpha and beta power is significantly larger in each active task as compared to the passive task (vertical dashed lines, Quade and Conover tests; $*p < .01$). (C) Topographic maps of the alpha (top) and beta (bottom) energy difference between the three active tasks pooled together and the passive task, at the respective latencies of maximal energy difference at C3. Central distribution of the energy decrease (black) is compatible with motor activity, although the motor response is diluted due to stimulus time-locked averaging.

There was a significant difference across the four tasks between 410 and 660 msec at electrode C3 due to a larger energy decrease in the three active tasks as compared to the passive task (Figure 7B). The beta power decrease obtained by measuring the difference between the three pooled active tasks and the passive task was centered on central electrodes, consistent with cerebral motor activity (Figure 7C).

DISCUSSION

Our study investigated the existence and nature of oscillatory activities during *n*-back working memory tasks with particular reference to the frequency range below 30 Hz. A previous work using comparable analysis tools analyzed the modulation of the 8–100 Hz oscillatory activity by memory, reporting induced gamma and beta oscillations during the delay of a visual short-term memory task (Tallon-Baudry et al., 1998). Our key addition to this study concerns the discrimination between the 3–30 Hz oscillatory activities related to stimulus perceptive and attentional processing and those associated with working memory per se. In order to separate the evoked from the induced oscillatory activities, we designed appropriate control tasks and quantified the phase-locking of the EEG signal to the stimulus. Our study included the theta frequency band, of major interest in working memory, and provided a precise topographical analysis of the oscillatory activities using surface Laplacian estimates, at the expense of a greater sensitivity to noise restraining the examination of high-frequency gamma oscillations.

Oscillatory Phase-locked Activity Related to Stimulus Perceptual Processing

The posterior EEG oscillations were phase-locked to the stimulus in theta, alpha, and beta frequency ranges. At low frequencies (theta band), the phase-locking component corresponded to stimulus duration, whereas at higher frequencies (alpha and beta bands), it followed stimulus onset and offset more closely. Such observations indicate that visual stimulus presentation may be mostly responsible for the early modulations of the 3–30 Hz EEG signal. The phase-locking component displayed similar features to the early P1–N1 complex of the ERPs, culminating at posterior sites and showing an OFF response at high frequencies. Recent studies have suggested that the superposition of evoked oscillations in the delta to beta range generate the early P1–N1 components of cortical ERPs (Gruber, Klimesch, Sauseng, & Doppelmayr, 2005; Klimesch et al., 2004).

In the theta frequency range, a transient energy increase was widely observed over the scalp within the 500 msec following stimulus onset. Such early rise of theta activity with respect to the stimulus has been previously reported (Krause et al., 2000; Tesche, & Karhu, 2000; Gevins et al., 1997), and is compatible with the cognitive gating phenomenon, theta activity turning on sharply during cognitive tasks and off between trials (Raghavachari et al., 2001). Although the constant stimulus presentation rate could be involved in the early modulation of theta activity, this is an unlikely hypothesis for several reasons. First, stimulus presentation frequency (0.2 Hz) was much smaller than theta frequency, excluding an entrainment phenomenon. Second, long interstimulus intervals (ISIs $\geq$5 sec) are known to reduce expectancy effects, the RTs being comparable to those observed in situations without a forewarning stimulus (Rohrbaugh et al., 1986). Third, the slow negative shift associated with expectancy and response preparation, classically developing within the delay period between two dependent stimuli (contingent negative variation, Tecce, & Cattanach, 1991), was absent in the ERPs (Figure 2). Most importantly, a separate analysis in an independent series of 10 subjects showed that the early theta energy during the detection task was similar using regular 5-sec ISI and variable 3.5- to 7.5-sec ISI. In addition, a methodological issue can partly account for the early rise of theta activity, as TF analysis tends to spread in time the spectral energy content of transient signals, especially in the low-frequency range, limiting their precise onset and offset determination.

The early transient theta activity was of larger amplitude at frontal sites, where it peaked slightly later than on parieto-occipital electrodes. In contrast to the parieto-occipital theta activity equally present in all tasks, the frontal theta activity was minimal in the passive viewing task, suggesting a different functional reactivity. Despite statistically nonnegligible phase-locked activity at frontal electrodes, the phase-locking values were significantly higher at parietal than at frontal sites, suggesting that the theta energy in the posterior region was largely phase-locked to the stimulus in contrast to the frontal region. This observation was supported by the analysis of latency correspondence between theta energy and phase-locking values, which revealed a good matching at the parietal electrode contrasting with a significant difference at the frontal electrode. Altogether, these findings demonstrate the phase-locked nature of the parieto-occipital theta energy, whereas the frontal theta energy is dominated by induced activity. Using an oscillatory phase resetting model, it has been recently shown that the posterior theta activity largely participated in the early components of the ERPs (Gruber et al., 2005; Klimesch et al., 2004), thus confirming the evoked nature of posterior theta activity. The interdependency of posterior theta power with visual evoked potentials was also observed through a parallel increase of both indices during visual stimuli presentation in warning and cue periods of a short-term memory task (Babiloni

et al., 2004). Consistent with our previous observations (Missonnier et al., 2003), the present tasks had no differential effect on the P1–N1 visual evoked potentials. These observations are in line with our finding that the posterior phase-locked theta energy is equally present in the four visual tasks and is not modulated by specific task demands. Yordanova et al. (2002) recently proposed that synchronization of ongoing theta oscillations could correspond to an obligatory processing stage for stimulus evaluation, as it was observed consistently across different stimulus modalities.

Oscillatory-induced Activity Related to Focused Attention

Although some phase-locked activity was still present, a major induced component of theta energy was identified in the frontal region. Frontal theta activity occurred with a large amplitude in the three active tasks as opposed to the passive task. In contrast to passive viewing, close attention to the stimulus was crucial for performance in the detection and *n*-back tasks, suggesting that the frontal transient theta component observed in the active tasks is tightly related to the focused attention requested for stimulus processing.

There is a substantial amount of evidence that frontal midline theta activity increases with mental effort, including concentration and focused attention (Aftanas & Golocheikine, 2001; Krause et al., 2000; Ishii et al., 1999; Kahana et al., 1999; Klimesch, 1999). However, the specific effect of attention on theta activity in the context of working memory tasks has been rarely explored. In a similar verbal working memory paradigm, Krause et al. (2000) observed a higher frontal theta ERS in the 4–6 Hz range after presentation of targets, especially in their 0-back condition functionally close to an attention task. This suggests that stimulus relevancy affects theta power magnitude even in simple detection tasks. A more direct evidence for implication of low-frequency oscillations in orienting response linked to focused attention was recently provided by the amplitude increase of a midfrontal 3-Hz component for task-relevant stimuli only (Onton et al., 2005). Although we did not directly compare target and nontarget trials in our experimental design, we found that for both trial types, frontal transient theta amplitude distinguished the three active tasks from the passive task. This result supports the hypothesis that the transient increase of frontal theta power is mainly linked to directed attention and is not affected by mnemonic processing.

Oscillatory-induced Activity Related to Working Memory

Within the 5000-msec delay interval between each letter presentation, we were able to identify sustained oscillatory activity in the theta (4–8Hz) and beta (15–25 Hz) frequency bands, which was higher for the more working memory-demanding, 2-back task. The very low phase-locking factor values observed in parallel confirmed the induced nature of these oscillations. Importantly, this induced activity was only seen in trials correctly recognized as nonmatching with task demand.

Theta Band

In the theta frequency range, energy remained sustained in the 2-back task between 965 and 2390 msec in the frontal region, including frontopolar electrodes. The sustained nature and anterior topographical distribution of these oscillations are consistent with the sustained prefrontal activation observed in neuroimaging data during working memory tasks (Owen et al., 1999; Cohen et al., 1997; Courtney et al., 1997; Manoach et al., 1997). Despite their methodological differences, previous studies have already suggested an increase of frontal theta power with memory load (Onton et al., 2005; Jensen et al., 2002; Jensen, & Tesche, 2002; Krause et al., 2000; Gevins et al., 1997). Krause et al. (2000) also observed a late and long lasting 6–8 Hz theta power over anterior sites that was stronger for the 2-back task. Consistent with our observations, this higher sustained theta energy in the 2-back task was only seen in nontarget trials. However, opposite results, namely, a sustained decrease of frontal and parietal theta power, have been reported in visuospatial working memory tasks (Babiloni et al., 2004; Bastiaansen, Posthuma, Groot, & de Geus, 2002), suggesting that domain-specific components of working memory may affect theta oscillations differently.

The present data go beyond Krause' findings in respect to three major points. First, they demonstrate for the first time, to our knowledge, a clear distinction between the early transient and the late sustained frontal theta component, the latter being the only one affected by memory load. Second, they identify the induced nature of the theta sustained oscillatory activity and specify its period of occurrence, providing important clues for interpreting its contribution to working memory process. Finally, they suggest that the working memory load effect on sustained theta activity is stronger over the midline and right frontal region, where the 2-back task elicited significantly more theta power than the 1-back task. The emergence of induced theta oscillatory activity modulated by memory load in our data is consistent with the hypothesis that memory performance could depend on cortico-hippocampal interactions at theta frequency (Newman, & Grace, 1999; Miller, 1991). Its presence restricted to nonmatched trials, as well as its time course of occurrence, suggests that it may subserve incremental retention and maintenance of new items for further task requirements (Tesche, & Karhu, 2000). Two arguments support this hypothesis. First, sustained induced theta activity for nonmatched

trials begins at 965 msec, that is, after the response in 2-back matched trials (RT = 837 ± 177 msec). Its temporal occurrence can thus be considered to be posterior to the comparative process between the incoming item and the memory buffer. Second, in the sequential letter presentation, two consecutive matches almost never occur (none in 1-back, 1 over 30 matches in 2-back), implying that after a matched response, the memory buffer is cleaned up and the retention process is not engaged. This could explain the absence of sustained theta activity in matched trials. The right midfrontal dominance of sustained theta energy in our 2-back task is compatible with the finding that within the prefrontal cortex, the right mid-dorsolateral region was specifically activated in relation to information update and manipulation into working memory (Owen et al., 1999). Additionally, an association between sustained frontal theta power and successful encoding of verbal items has recently been observed, the right hemisphere being predominantly involved when complete information (i.e., item and context) is successfully encoded (Summerfield, & Mangels, 2005).

The absence of a significant difference in sustained theta activity between detection and 1-back tasks is consistent with the observations of Krause et al. (2000) and indicated that a certain level of memory demand is necessary to trigger scalp-recordable theta reactivity. Various studies have suggested that theta activity could be related to the level of mental effort necessary to deal with the task rather than the amount of information being manipulated or the immediate cognitive demand (Onton et al., 2005; Caplan, Madsen, Raghavachari, & Kahana, 2001; McEvoy, Pellouchoud, Smith, & Gevins, 2001). Although the issue remains difficult to resolve because task difficulty is intrinsically linked to the highest memory load, our own as well as others' data did not reveal a linear modulation of theta magnitude with memory load (Krause et al., 2000; Gevins et al., 1997), supporting a general effect of task demand. An alternative explanation is that our detection and 1-back conditions did not fundamentally differ in terms of task requirement. Further experimental strategies, including separate control of task complexity and memory load, would help to clarify the issue.

Beta Band

Our data also revealed a sustained beta activity sensitive to memory load largely present in the parietal region, starting at 1200 msec and lasting for 1000 msec. In contrast to the gamma range, the beta frequency range has been seldom explored in relation to working memory. Tallon-Baudry et al. (1998) observed a sustained memory-related enhancement of the 15–20 Hz energy in the occipital region that was more pronounced on the right side, whereas in the medial and right frontal region a shorter lasting beta component was identified. More recently, a discrete increase of low beta power (12–16 Hz) was also observed in the frontocentral region during memory encoding (Onton et al., 2005). Our own data additionally demonstrate the reactivity of the beta rhythm to the verbal working memory load, more pronounced in the right parietal region. We did not replicate the discrete frontal beta power increase identified in previous studies (Onton et al., 2005; Tallon-Baudry et al., 1998), possibly because of task differences more likely to affect subtle modulation of oscillatory activity. The period of induced beta occurrence suggests that it could be related to active maintenance of new items in memory, as for induced sustained theta activity. Such interpretation is compatible with recent reports of stronger low beta activity during presentation of letters to add to the rehearsal string as compared to letters to ignore (Onton et al., 2005). The parietal distribution of beta energy matches neuroimaging data reporting the involvement of bilateral parietal regions in verbal working memory (Cohen et al., 1997; Manoach et al., 1997; Smith, & Jonides, 1997). Various interpretation for right parietal predominance in verbal working memory tasks have been proposed, including right parietal contribution to domain-general (i.e., selective attention) or domain-specific functions (i.e., visuospatial coding or recognition of visually presented letters) (Ravizza, Behrmann, & Fiez, 2005). The higher right parietal beta energy that we observed in the 2-back task could reflect enhanced attention driven by the more demanding task (Corbetta, & Shulman, 2002). Moreover, we demonstrated that memory-related beta activity was independent of motor-related beta activity. Beta activity related to working memory consisted of an energy increase in the parietal region, restricted to the trials without motor response. In contrast, motor-related beta activity observed only in response trials was revealed by a decrease in energy in the central region, as classically described (Pfurtscheller, Pregenzer, & Neuper, 1994; Pfurtscheller, 1981).

Independently of working memory processing, earlier and larger parietal beta synchronization was observed in the three active tasks as compared to the passive task. This observation supports the implication of beta oscillations into large-scale processes tuning cortical excitability for specific neural processing (Neuper & Pfurtscheller, 2001; Pfurtscheller, 2001). The present data also showed earlier beta synchronization in the detection task as compared to the *n*-back tasks in nonresponse trials. This finding supports the hypothesis that cortical processing for simple item identification is faster than for memory match-to-sample item identification. However, the fact that this difference in processing time occurred only for items identified as nontargets suggests that it is limited to the rejection process, which also includes motor inhibition. Response-locked analysis could contribute to a better understanding of these findings.

Alpha Band

In contrast to most reports, we did not find any evidence of significant modulation of alpha activity in our working memory tasks. A long lasting decrease of alpha power was observed in the three active tasks, particularly large in trials including motor response, followed by a late power rebound. It is well known that motor preparatory and executive processing blocks alpha activity in the central region (for review, Kristeva-Feige, Feige, Makeig, Ross, & Elbert, 1993). While confirming this fact, we did not find evidence for cognitive modulation on the magnitude of alpha power decrease or on the late alpha power rebound. The absence of working memory effect on alpha rhythm has already been described (Tallon-Baudry et al., 1998). Nevertheless, a decrease of alpha power with task demand was previously reported by most, although topography and/or affected frequency range varies considerably among studies (Babiloni et al., 2004; Krause et al., 2000; Klimesch, 1999; Gevins et al., 1997). In apparent conflict with these findings, other studies have described an increase of alpha power with task demand (Herrmann, Senkowski, & Rottger, 2004; Bastiaansen et al., 2002; Jensen et al., 2002; Krause et al., 2000; Klimesch, Doppelmayr, Schwaiger, Auinger, & Winkler, 1999). The decrease of alpha activity is supposedly related to enhanced efficiency of information transfer within thalamocortical pathways, resulting in an increase of attention and/or memory performance (Babiloni et al., 2004; Klimesch, 1999). The increase of alpha activity could reflect active inhibition in order to prevent the information flow into areas retaining memory items, but could also be directly related to working memory maintenance (Jensen et al., 2002; Klimesch et al., 1999). Although the issue remains unsolved, it cannot be ruled out that the overlap of opposite effects induced by the combination of various experimental factors may have canceled out the net reactivity of alpha energy.

Conclusion

Our study made it possible to identify various oscillatory patterns at distinct frequencies and time during *n*-back working memory tasks. The earliest emergent oscillatory activity occurred during stimulus presentation and consisted in a transient increase of theta energy widely distributed over the scalp. In the posterior region, theta power was phase-locked to the stimulus, whereas in the frontal region, phase-locked and induced theta activity overlapped, the latter dominating the net theta energy. The amplitude of frontal theta activity depended on the attention level required to perform the task, suggesting that the anterior component of the distributed attention network could be implicated in its generation. Working memory load modulated induced oscillatory activity in a sustained manner in both theta and beta frequency ranges. Larger theta and beta power was observed during the most demanding 2-back task after item classification as nontarget had taken place, suggesting that these oscillations coincided with storage and active maintenance of the current item for further task demands. Interestingly, the distribution of theta and beta induced activities differed, the slow oscillations having a frontal topography contrasting with the parietal distribution of the higher frequency oscillations. The modulation of frontal and parietal oscillations is consistent with the implication of a fronto-parietal network in working memory reported by neuroimaging studies (Baddeley, 1998; Cohen et al., 1997; Manoach et al., 1997). How these spectrally distributed oscillations are integrated to support working memory remains an open issue. Recent data have suggested that cross-frequency synchrony, shown to be modulated by cognitive task demand, could play a major role in such an integration (Palva, Palva, & Kaila, 2005). Frontal theta activity is compatible with activation of cortico-hippocampal loops for storage and retrieval of cortically represented memories, whereas high-frequency parietal activity could underlie the cortical maintenance of mnemonic representations in a form accessible to short-term decision-making process. Further exploration of intra- and cross-spectral synchrony is required to better delineate the interactive role of these oscillatory activities into working memory processing.

Acknowledgments

This project was funded by the Swiss National Foundation for Scientific Research, grant 3100A0/103770/1; the Research and Development Hospital, grant 02-1-122; as well as by unrestricted grants from the Novartis Foundation, Ernst and Lucie Schmidheiny Foundation, and Stiftung für Klinische Neuropsychiatrische Forschung.

Reprint requests should be sent to Marie-Pierre Deiber, Hôpitaux Universitaires de Genève, Service de Neuropsychiatrie, Unité de Neuroimagerie, Chemin du Petit-Bel-Air 2, CH-1225 Chene-Bourg, Geneva, Switzerland, or via e-mail: Marie.P.DeiberIbanez@hcuge.ch.

REFERENCES

Aftanas, L. I., & Golocheikine, S. A. (2001). Human anterior and frontal midline theta and lower alpha reflect emotionally positive state and internalized attention: High-resolution EEG investigation of meditation. *Neuroscience Letters, 310,* 57–60.

Babiloni, C., Babiloni, F., Carducci, F., Cappa, S. F., Cincotti, F., Del Percio, C., et al. (2004). Human cortical responses during one-bit short-term memory. A high-resolution EEG study on delayed choice reaction time tasks. *Clinical Neurophysiology, 115,* 161–170.

Babiloni, F., Babiloni, C., Carducci, F., Fattorini, L., Onorati, P., & Urbano, A. (1996). Spline laplacian estimate of EEG potentials over a realistic magnetic resonance-constructed scalp surface model. *Electroencephalography and Clinical Neurophysiology, 98,* 363–373.

Baddeley, A. (1998). Recent developments in working memory. *Current Opinion in Neurobiology, 8,* 234–238.
Bastiaansen, M., & Hagoort, P. (2003). Event-induced theta responses as a window on the dynamics of memory. *Cortex, 39,* 967–992.
Bastiaansen, M. C., Posthuma, D., Groot, P. F., & de Geus, E. J. (2002). Event-related alpha and theta responses in a visuo-spatial working memory task. *Clinical Neurophysiology, 113,* 1882–1893.
Caplan, J. B., Madsen, J. R., Raghavachari, S., & Kahana, M. J. (2001). Distinct patterns of brain oscillations underlie two basic parameters of human maze learning. *Journal of Neurophysiology, 86,* 368–380.
Cohen, J. D., Perlstein, W. M., Braver, T. S., Nystrom, L. E., Noll, D. C., Jonides, J., et al. (1997). Temporal dynamics of brain activation during a working memory task. *Nature, 386,* 604–608.
Conover, W. J. (1980). *Practical nonparametric statistics.* New York: Wiley.
Corbetta, M., & Shulman, G. L. (2002). Control of goal-directed and stimulus-driven attention in the brain. *Nature Reviews Neuroscience, 3,* 201–215.
Courtney, S. M., Ungerleider, L. G., Keil, K., & Haxby, J. V. (1997). Transient and sustained activity in a distributed neural system for human working memory. *Nature, 386,* 608–611.
Gevins, A., Smith, M., McEvoy, L., & Yu, D. (1997). High-resolution EEG mapping of cortical activation related to working memory: Effects of task difficulty, type of processing, and practice. *Cerebral Cortex, 7,* 374–385.
Grossmann, A., Kronland-Martinet, R., & Morlet, J. (1989). Reading and understanding continuous wavelets transforms. In J. M. Combes, A. Grossmann, & P. Tchamitchian (Eds.), *Wavelet, time–frequency methods and phase space* (pp. 2–20). Berlin: Springer.
Gruber, T., Tsivilis, D., Montaldi, D., & Muller, M. M. (2004). Induced gamma band responses: An early marker of memory encoding and retrieval. *NeuroReport, 15,* 1837–1841.
Gruber, W. R., Klimesch, W., Sauseng, P., & Doppelmayr, M. (2005). Alpha phase synchronization predicts P1 and N1 latency and amplitude size. *Cerebral Cortex, 15,* 371–377.
Herrmann, C. S., Munk, M. H. J., & Engel, A. K. (2004). Cognitive functions of gamma-band activity: Memory match and utilization. *Trends in Cognitive Sciences, 8,* 347–355.
Herrmann, C. S., Senkowski, D., & Rottger, S. (2004). Phase-locking and amplitude modulations of EEG alpha: Two measures reflect different cognitive processes in a working memory task. *Experimental Psychology, 51,* 311–318.
Howard, M. W., Rizzuto, D. S., Caplan, J. B., Madsen, J. R., Lisman, J., Aschenbrenner-Scheibe, R., et al. (2003). Gamma oscillations correlate with working memory load in humans. *Cerebral Cortex, 13,* 1369–1374.
Ishii, R., Shinosaki, K., Ukai, S., Inouye, T., Ishihara, T., Yoshimine, T., et al. (1999). Medial prefrontal cortex generates frontal midline theta rhythm. *NeuroReport, 10,* 675–679.
Jensen, O., & Tesche, C. D. (2002). Frontal theta activity in humans increases with memory load in a working memory task. *European Journal of Neuroscience, 15,* 1395–1399.
Jensen, O., Gelfand, J., Kounios, J., & Lisman, J. E. (2002). Oscillations in the alpha band (9–12 Hz) increase with memory load during retention in a short-term memory task. *Cerebral Cortex, 12,* 877–882.
Jervis, B. W., Nichols, M. J., Johnson, T. E., Allen, E., & Hudson, N. R. (1983). A fundamental investigation of the composition of auditory evoked potentials. *IEEE Transactions on Biomedical Engineering, 30,* 43–50.
Kahana, M. J., Sekuler, R., Caplan, J. B., Kirschen, M., & Madsen, J. R. (1999). Human theta oscillations exhibit task dependence during virtual maze navigation. *Nature, 399,* 781–784.
Klimesch, W. (1999). EEG alpha and theta oscillations reflect cognitive and memory performance: A review and analysis. *Brain Research Reviews, 29,* 169–195.
Klimesch, W., Doppelmayr, M., Schwaiger, J., Auinger, P., & Winkler, T. (1999). ''Paradoxical'' alpha synchronization in a memory task. *Cognitive Brain Research, 7,* 493–501.
Klimesch, W., Russegger, H., Doppelmayr, M., & Pachinger, T. (1998). A method for the calculation of induced band power: Implications for the significance of brain oscillations. *Electroencephalography and Clinical Neurophysiology, 108,* 123–130.
Klimesch, W., Schack, B., Schabus, M., Doppelmayr, M., Gruber, W., & Sauseng, P. (2004). Phase-locked alpha and theta oscillations generate the P1–N1 complex and are related to memory performance. *Cognitive Brain Research, 19,* 302–316.
Krause, C. M., Sillanmaki, L., Koivisto, M., Saarela, C., Haggqvist, A., Laine, M., et al. (2000). The effects of memory load on event-related EEG desynchronization and synchronization. *Clinical Neurophysiology, 111,* 2071–2078.
Kristeva-Feige, R., Feige, B., Makeig, S., Ross, B., & Elbert, T. (1993). Oscillatory brain activity during a motor task. *NeuroReport, 4,* 1291–1294.
Kronland-Martinet, R., Morlet, J., & Grossmann, A. (1987). Analysis of sound patterns through wavelet transforms. *International Journal of Pattern Recognition and Artificial Intelligence, 1,* 273–302.
Manoach, D. S., Schlaug, G., Siewert, B., Darby, D. G., Bly, B. M., Benfield, A., et al. (1997). Prefrontal cortex fMRI signal changes are correlated with working memory load. *NeuroReport, 8,* 545–549.
McEvoy, L. K., Pellouchoud, E., Smith, M. E., & Gevins, A. (2001). Neurophysiological signals of working memory in normal aging. *Cognitive Brain Research, 11,* 363–376.
Miller, R. (1991). *Cortico-hippocampal interplay and the representation of contexts in the brain.* Berlin: Springer-Verlag.
Missonnier, P., Leonards, U., Gold, G., Palix, J., Ibanez, V., & Giannakopoulos, P. (2003). A new electrophysiological index for working memory load in humans. *NeuroReport, 14,* 1451–1455.
Neuper, C., & Pfurtscheller, G. (2001). Event-related dynamics of cortical rhythms: Frequency-specific features and functional correlates. *International Journal of Psychophysiology, 43,* 41–58.
Newman, J., & Grace, A. A. (1999). Binding across time: The selective gating of frontal and hippocampal systems modulating working memory and attentional states. *Consciousness and Cognition, 8,* 196–212.
Onton, J., Delorme, A., & Makeig, S. (2005). Frontal midline EEG dynamics during working memory. *Neuroimage, 27,* 341–356.
Owen, A. M., Herrod, N. J., Menon, D. K., Clark, J. C., Downey, S. P., Carpenter, T. A., et al. (1999). Redefining the functional organization of working memory processes within human lateral prefrontal cortex. *European Journal of Neuroscience, 11,* 567–574.
Palva, J. M., Palva, S., & Kaila, K. (2005). Phase synchrony among neuronal oscillations in the human cortex. *Journal of Neuroscience, 25,* 3962–3972.
Perrin, F., Bertrand, O., & Pernier, J. (1987). Scalp current density mapping: Value and estimation from potential

data. *IEEE Transactions on Biomedical Engineering, 34,* 283–288.
Pfurtscheller, G. (1981). Central beta rhythm during sensorimotor activities in man. *Electroencephalography and Clinical Neurophysiology, 51,* 253–264.
Pfurtscheller, G. (2001). Functional brain imaging based on ERD/ERS. *Vision Research, 41,* 1257–1260.
Pfurtscheller, G., Pregenzer, M., & Neuper, C. (1994). Visualization of sensorimotor areas involved in preparation for hand movement based on classification of mu and central beta rhythms in single EEG trials in man. *Neuroscience Letters, 181,* 43–46.
Raghavachari, S., Kahana, M. J., Rizzuto, D. S., Caplan, J. B., Kirschen, M. P., Bourgeois, B., et al. (2001). Gating of human theta oscillations by a working memory task. *Journal of Neuroscience, 21,* 3175–3183.
Ravizza, S. M., Behrmann, M., & Fiez, J. A. (2005). Right parietal contributions to verbal working memory: Spatial or executive? *Neuropsychologia, 43,* 2057–2067.
Rohrbaugh, J. W., McCallum, W. C., Gaillard, A. W., Simons, R. F., Birbaumer, N., & Papakostopoulos, D. (1986). ERPs associated with preparatory and movement-related processes. A review. *Electroencephalography and Clinical Neurophysiology—Supplement, 38,* 189–229.
Sederberg, P. B., Kahana, M. J., Howard, M. W., Donner, E. J., & Madsen, J. R. (2003). Theta and gamma oscillations during encoding predict subsequent recall. *Journal of Neuroscience, 23,* 10809–10814.
Smith, E. E., & Jonides, J. (1997). Working memory: A view from neuroimaging. *Cognitive Psychology, 33,* 5–42.
Summerfield, C., & Mangels, J. A. (2005). Coherent theta-band EEG activity predicts item–context binding during encoding. *Neuroimage, 24,* 692–703.
Tallon-Baudry, C., & Bertrand, O. (1999). Oscillatory gamma activity in humans and its role in object representation. *Trends in Cognitive Sciences, 3,* 151–162.
Tallon-Baudry, C., Bertrand, O., Delpuech, C., & Pernier, J. (1996). Stimulus specificity of phase-locked and non-phase-locked 40 Hz visual responses in human. *Journal of Neuroscience, 16,* 4240–4249.
Tallon-Baudry, C., Bertrand, O., Delpuech, C., & Permier, J. (1997). Oscillatory gamma-band (30–70 Hz) activity induced by a visual search task in humans. *Journal of Neuroscience, 17,* 722–734.
Tallon-Baudry, C., Bertrand, O., & Fischer, C. (2001). Oscillatory synchrony between human extrastriate areas during visual short-term memory maintenance. *Journal of Neuroscience, 21,* RC177.
Tallon-Baudry, C., Bertrand, O., Peronnet, F., & Pernier, J. (1998). Induced gamma-band activity during the delay of a visual short-term memory task in humans. *Journal of Neuroscience, 18,* 4244–4254.
Tecce, J. J., & Cattanach, L. (1991). Contingent negative variation. In E. Niedermeyer & F. Lopes da Silva (Eds.), *Electroencephalography: Basic principles, clinical applications and related fields* (pp. 887–910). Munich: Urban and Schwarzenberg.
Tesche, C. D., & Karhu, J. (2000). Theta oscillations index human hippocampal activation during a working memory task. *Proceedings of the National Academy of Sciences, U.S.A., 97,* 919–924.
Yordanova, J., Kolev, V., Rosso, O. A., Schurmann, M., Sakowitz, O. W., Ozgoren, M., et al. (2002). Wavelet entropy analysis of event-related potentials indicates modality-independent theta dominance. *Journal of Neuroscience Methods, 117,* 99–109.